Available online at www.sciencedirect.com
ScienceDirect
Coordination Chemistry Reviews 252 (2008) 259–272
COORDINATION CHEMISTRY REVIEWS
www.elsevier.com/locate/ccr

Review

Primary photochemistry and energetics leading to the oxidation of the (Mn)4Ca cluster and to the evolution of molecular oxygen in Photosystem II

Fabrice Rappaport [a,*], Bruce A. Diner [b,**]

[a] *Institut de Biologie Physico-Chimique, UMR7141 CNRS-Université Pierre et Marie Curie, 13 rue Pierre et Marie Curie, 75005 Paris, France*
[b] *CR&D, Experimental Station, E. I. du Pont de Nemours & Co., Wilmington, DE 19880-0173, USA*

Received 29 March 2007; accepted 26 July 2007
Available online 2 August 2007

Contents

Abbreviations: DCMU: diuron, 3-(3,4-dichlorophenyl)-1,1-dimethylurea; Chl_{D1}; Chl_{D2}, the two monomeric chlorophylls located, respectively, between the P_{D1}/P_{D2} special pair and $Pheo_{D1}$ and $Pheo_{D2}$ and bound to the D1 and D2 subunits; e^-, electron; H^+, proton; $Pheo_{D1}$; $Pheo_{D2}$, the two pheophytins *a* bound, respectively, to the D_1 and D_2 subunits of PSII; P_{D1}; P_{D2}, the two chlorophylls *a* forming the "special pair" and bound, respectively, to the D_1 and D_2 subunits of PSII; P_L; P_M, the two bacteriochlorophylls forming the "special pair" and bound, respectively, to the L and M subunits of the purple bacterial reaction center; PSII, photosystem II; Q_A and Q_B, the primary and secondary plastoquinone-9 electron acceptors; RC, reaction center; RP, radical pair; Y_Z, D1-Tyr161 the redox-active tyrosine of PSII on the D1 polypeptide; Y_D; D2-Tyr160, the redox-active tyrosine of PSII on the D2 polypeptide

* Corresponding author. Tel.: +33 1 584 150 59; fax: +33 1 584 150 22.
** Corresponding author. Tel.: +1 302 695 2494; fax: +1 302 695 9183.
E-mail addresses: Fabrice.Rappaport@ibpc.fr (F. Rappaport),Bruce.A.Diner@usa.dupont.com (B.A. Diner).

doi:10.1016/j.ccr.2007.07.016

Abstract

The recent availability of X-ray crystallographic structures of Photosystem II (PSII) together with refined steady-state and time-resolved spectroscopic analyses of site-directed mutants, are leading to a more detailed understanding of the function of this photosystem. Recent data have significantly modified the energetic picture of Photosystem II: the midpoint potentials of the first redox carriers in the chain leading to water-splitting have been reevaluated, the free-energy changes associated with the subsequent electron/proton transfer steps have been estimated and, last but not least, the free-energy landscape of the water-splitting reaction is starting to emerge with the identification of reaction intermediates and the free-energy changes associated with the formation of these transient species.

Keywords: Photosystem II; Chlorophyll; Photochemistry; Energetics; Water oxidation

1. Introduction

The oxidation of water to molecular oxygen is described by the equation: $2H_2O \rightarrow O_2 + 4H^+ + 4e^-$. Water is a very stable molecule and its oxidation requires the availability of strongly oxidizing species (at pH 7.0 the midpoint potential of the $O_2/2H_2O$ couple is 810 mV). In Photosystem II (PSII), the only biological complex capable of producing oxygen from water, this oxidizing power is provided by the successive absorption of four photons and their photochemical conversion into electrochemical energy. PS II bears various redox cofactors among which are: a chlorophyll *a* dimer ($P_{D1}P_{D2}$), two chlorophyll *a* monomers (Chl_{D1} and Chl_{D2}), two pheophytins *a* ($Pheo_{D1}$ and $Pheo_{D2}$), two plastoquinones Q_A and Q_B, two redox-active tyrosines and a tetranuclear manganese cluster. An absorbed photon is used to promote an electron from the ground to the excited state of a redox-active chlorophyll. This electron is now a strong reductant and is transferred to a nearby acceptor. The resulting charge-separated state is then further stabilized by successive electron transfer steps involving multiple redox centers. The coupling between this one-electron process and the oxidation of water to dioxygen, a four-electron process, is made possible by a charge-storing mechanism in PSII which allows the accumulation in one site of the four oxidizing equivalents needed to generate molecular oxygen. This catalytic center, composed of four Mn ions and one Ca ion coordinated by μ-oxo bridges and amino-acid residues, has five different oxidation states (S_0, S_1, S_2, S_3 and S_4). Four successive light reactions drive the four successive oxidations between the S_i and S_{i+1} states [1,2]. Upon S_4 formation, an oxygen molecule is produced and released, regenerating the S_0 state. The success of this model, first proposed by Bessel Kok, resides in its ability to formally and simply describe the function of the enzyme without any assumptions as to the chemical nature of the transient states involved, nor on the precise mechanisms underlying the interconversion of the S states. Numerous studies aimed at unraveling the structure and function of PSII, now allow one to go far beyond this phenomenological description. We attempt here to review some of the recent progress in the understanding of the mechanisms and energetics which underlie photosynthetic water oxidation.

2. Primary charge separation: structural arrangement of the cofactors and mechanism

2.1. A brief comparison of PSII with purple bacterial RCs

The arrangement of the redox cofactors in PSII reaction centers is quite close to that of the purple bacterial reaction centers, with two parallel A and B branches that span the photosynthetic membrane (see Fig. 1). The similar distances and orientations of these components and the homology between the L and M and D1 and D2 subunits that coordinate them led to the initial expectation that the kinetics and mechanism of primary charge separation would be very similar (discussed in [3] and see [4–8,13,23] for structures). There are, however, a number of structural modifications that likely contribute to the observed

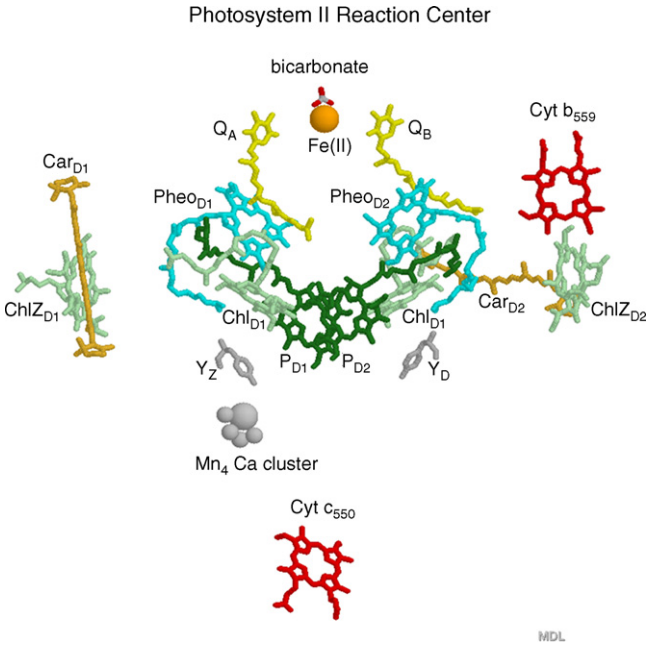

Fig. 1. Redox-active components of the *Thermosynechococcus elongatus* Photosystem II adapted from [13] (pdb datafile: 2AXT). The view is in the plane of the membrane. The subscript D_1 or D_2 refers to the subunit which binds the redox components.

kinetic and mechanistic differences to be described below. Certainly, the major difference is the replacement of Bchlorophyll *a* with chlorophyll *a*, Bpheophytin *a* with pheophytin *a* and ubiquinone with plastoquinone. Other differences include the electronic interaction coupling between the special pair chlorophylls, 500–1000 cm^{-1} [9] for P_L and P_M in the purple bacterial RCs and 85–140 cm^{-1} [10–12] for P_{D1} and P_{D2} in PSII. These likely arise from differences in the center to center distances, 7.4–7.6 Å for P_L and P_M [4] versus 7.6–8.4 for P_{D1} and P_{D2} [8,13], side to side separation and a slightly different orientation of the tetrapyrrole head groups, all of which affect orbital overlap. The electronic coupling between P_L and P_M in the bacterial reaction centers produces a substantial low energy exciton band, the longest wavelength band of the reaction center, resulting in the direction of excitation energy to the P_LP_M special pair. In PSII, the much weaker coupling between the reaction center pigments makes for much less spectral differentiation between the reaction center chlorins. The Chl_{D1} and Chl_{D2} accessory chlorophylls in PSII lack the axial histidine ligands that coordinate their bacterial reaction center homologues (L-His153 and M-His180 (*R. viridis* numbering) replaced by Thr179 and Ile178, respectively) and are likely coordinated by water molecules, though these are not actually visible at the current resolution of the X-ray structures [6–8,13,23]. The significance of this difference is not entirely clear, though it could affect the reduction potentials of these chlorophylls.

2.2. A-branch electron transfer

In the case of the purple bacterial reaction centers, charge separation is initiated at the special pair Bchlorophylls P_L and P_M to form P^+Pheo^- with electron transfer occurring on the so-called A-branch (L-side) of the reaction center. There is a clear-cut preference for A-branch (D1-side) electron transfer in PSII as well. Of the two pheophytins associated with the PSII reaction center, $Pheo_{D1}$ is the more likely primary acceptor as it is located on the active A-branch of the reaction center in close proximity to the primary quinone electron acceptor, Q_A. Direct evidence for the D1-side (PSII A-branch) pheophytin, $Pheo_{D1}$, in this role is provided by spectroscopic signals (ENDOR, Resonance Raman and FTIR) associated with the perturbation of the hydrogen bond to the $C_{13}{}^1$=O keto carbonyl of $Pheo_{D1}$ from residue D1-130, homologous to the L-104 hydrogen bond to the active branch pheophytin of the purple bacterial reaction centers [14–16]. Site directed mutations, D1-Gln130Glu and Leu, in *Synechocystis* 6803 shift the absorbance spectrum of the $P_{680}{}^+Pheo^-$ radical pair state [17] and lower and raise, respectively, the energy of the $P_{680}{}^+Pheo^-$ radical pair state by 34 and by 53 meV, respectively, measured at 60 ps following actinic excitation [18]. Similar values were recently obtained by comparing the intensity of the thermoluminescence band associated with $S_2Q_A{}^-$ charge recombination, in the WT and mutant strains [19]. Site-directed mutations in *Chlamydomonas reinhardtii* at D1-Glu130His, Gln and Leu shift the value of the gx component of the g-tensor for $Pheo^-$ as detected by high-field EPR [20]. Given the small energy differences in the optical transitions of the A and B branch monomeric accessory chlorophylls and pheophytins, it is likely that the preference for the A branch at room temperature has to do with the energetics of formation of the primary radical pair, the anion of which is a $Pheo^-$ (see below). Ishikata et al. [21], for example have calculated, based on the X-ray crystallographic structures, reduction potentials of −499 and −577 mV for the A- and B-branch Pheo's, respectively. Were the A- and B-branch accessory chlorophylls to have equivalent reduction potentials, then the A-branch would be highly favored. However, depending on the structural model used, these authors [22] estimate that one or the other of the two accessory chlorophylls has the lower reduction potential out of the four chlorophylls centrally located in the reaction center. Experimental evidence, however, indicates that the cation is stabilized primarily on P_{D1} (see below), which implies either that the X-ray crystallographic models used [8,23] are not yet sufficiently well-resolved to accurately compute the reduction potentials of the accessory chlorophylls or that the assumptions regarding their electrostatic environment are not altogether accurate.

2.3. Radical pair states and implication of Chl_{D1} in primary radical pair formation

Several groups have argued, based on the following observations, that charge separation in PSII is initiated on Chl_{D1} rather than on P_{D1} and P_{D2}. This evidence includes (1) special conditions under which direct excitation of B_A (the bacterial homolog of Chl_{D1}) was achieved in bacterial reaction centers, initiating charge separation from this chromophore despite the normal preference for excitation energy localization on the excitonically coupled P_L and P_M Bchlorophylls [24–26]. Because the excited states in the PSII reaction center are more degenerate, the probability of such charge separation occurring from Chl_{D1} was suggested to be higher [11,27–31], and even favored at low temperature where Chl_{D1} is the red-most chlorophyll of the reaction center [3,32]; (2) interpretation of coherent photon echo spectroscopy experiments [30]; (3) interpretation of Stark spectra as indicating the existence of a $Chl_{D1}{}^{\delta+}Pheo^{\delta-}$ charge-transfer state [33], and (4) detection of a $Pheo^-$, formed in the initial radical pair state prior to the detection of $P_{680}{}^+$ (cation mostly resides on P_{D1}, see below), implying that the cation involved in the initial charge pair with $Pheo^-$ is located on a redox species at higher energy and closer than P_{D1}, most likely an accessory chlorophyll [34,35].

2.4. Kinetics of radical pair formation

Measurements of charge separation in PSII (see Fig. 2) are quite complicated and multiphasic owing in part to the difficulty in distinguishing between absorbance changes associated with excited states and radical pair states which tend to be nearly isoenergetic, coupled with inhomogeneous optical broadening, a distribution of energy levels of each of multiple radical pair states, including those coupled to protein relaxation. The interpretation of the results also depends on how one models the spectral components, including exciton coupling and how one calculates intrinsic rate constants from the measured or effective rate constants. These issues become even more complex

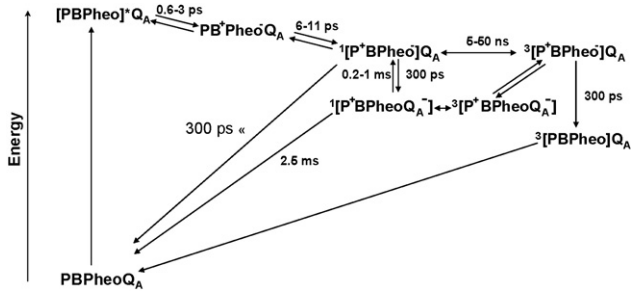

Fig. 2. Electron transfer dynamics in Photosystem II: the electron acceptor side. See text for a detailed discussion.

the larger the size of the antenna complex associated with the reaction center. A discussion of these issues and how they relate to the kinetics of formation of the primary radical pair, ranging from subpicosecond to ~20 ps at room temperature, are reviewed in the following references [29,36,37]. Recent publications using femtosecond infrared and visible absorbance spectroscopy ($T \geq 4\,^{\circ}C$) provide quite different numbers in D1-D2-cyt*b*559 reaction centers isolated from spinach, though both agree that $Pheo_{D1}^{-}$ is formed in the initial radical pair state. Groot et al. [34] using infrared spectroscopy detect $Pheo^{-}$ (RP1) in 0.6–0.8 ps while P_{680}^{+} (RP2) appears with a lifetime of ~6 ps. Holzwarth et al. [35] working at ambient temperature in the visible range find that the initial radical pair state containing $Pheo^{-}$ (RP1) appears in 3.2 ps while state $P_{680}^{+}Pheo^{-}$ appears with a lifetime of 11 ps. In core complexes, these lifetimes are similar at 1.4 and 8 ps, respectively. A relaxed $P_{680}^{+}Pheo^{-}$ state is suggested to form in 135 ps in reaction centers lacking Q_A while in core complexes a 202 ps lifetime is attributed to the formation of radical pair $P_{680}^{+}Q_A^{-}$, the latter being typical of the 200–500 ps reported for electron transfer from $Pheo^{-}$ to Q_A (see [36] for relevant references). Both groups agree that $Pheo^{-}$ appears prior to P_{680}^{+} and attribute the oxidized donor in RP1 to Chl_{D1}^{+}. With regard to this issue, PSII would significantly differ from its bacterial homolog in which, according to the favored sequence of events, the primary electron donor is P and the primary electron acceptor the "accessory" (Chl_{D1}).

2.5. Photosystem I, Photosystem II and Type II bacterial reaction centers—which is the odd one out?

Interestingly enough, it has been proposed recently that a similar charge separation mechanism applies in Photosystem I. This comes from the finding that mutation near P_{700} affects the rate of the RP1–RP2 step rather than that of the formation of the first radical pair (RP1) [38]. In line with this, in Photosystem I, mutations near the ec_3-A or ec_3-B Chls, which are structurally analogous to $Pheo_{D1}$ or $Pheo_{D2}$ in PSII, affect the relative efficiency for electron transfer down the A- or B-branch in a complementary manner [39]. This observation was taken as an indication that these chlorophylls are involved in the initial charge-separation mechanism [39]. In PSI, the rings of the ec2 and ec3 chlorophylls are almost parallel and partially overlap [40], whereas, as discussed above, the structural arrangement of the redox cofactors in PSII and type II bacterial RCs are similar, with the tetrapyrrole head groups of the Chl and Pheo oriented at an angle of ~45°. Yet, although structurally similar to the bacterial RC, PSII thus seems to be functionally more closely related to PSI. A feature that is common to PSII and PSI and different from the bacterial RCs is the relatively weak coupling between the six chlorins participating in the primary and secondary electron transfer steps (see above and [41,42]), so that this ensemble may be seen as a multimer of the six nearly equally coupled chlorins [43–45]. In the case of PSII, it has been put forward that such a multimeric organization would be a key feature in determining the tuning of the photochemical trapping efficiency and the control of the excitonic flux by the quenching of the exciton in the antenna [44]. Indeed, it would reconcile two apparently conflicting requirements, the need for a slow enough charge separation rate to allow, under certain conditions (e.g. under high light stress), the efficient quenching of the exciton within the antenna complexes and the achievement of a high quantum yield [44]. Although exciton quenching is thought to occur mostly within the PSII light harvesting complexes, long wavelength absorbing chlorophylls associated with PSI could be involved in the regulation of the exciton flux, provided that, as in the PSII case, their deexcitation can compete with charge separation. It is thus tempting to propose that the reasons for the "shifted", with respect to the bacterial reaction center case, charge separation mechanism which is common to PSI and PSII, lie in the weak coupling between the Chls constituting the P_{680} or P_{700} dimers.

2.6. Localization of the P_{680}^{+} cation

FTIR detection of an intervalence near IR band (2000–3000 cm^{-1}) [46,47] and ENDOR measurements of methyl hyperfine couplings [48,49] have been interpreted as indicating some delocalization of the P_{680}^{+} cation between P_{D1} and P_{D2}. The ENDOR measurements were suggested to indicate an approximate 80:20 distribution, though such measurements could not indicate which of the chlorophylls dominated. Site-directed mutations at D1-His198 and D2-His197, the axial ligands of P_{D1} and P_{D2}, respectively, were able to introduce displacements of the absorbance spectra in both the Soret and Qy absorbance bands and in some cases changes in the reduction potential of P_{680}^{+}/P_{680} [32]. The displacement of the spectra was larger and to the blue for site-directed mutations at D1-His198, consistent with the replacement of the polarizable His ligand with the less polarizable Gln, Asn or Ala (actually a water). The consequences of the mutations constructed at D1-His197 tended to be smaller, showing small shifts to the red in those cases where the Chl^{+}/Chl reduction potential decreased, suggesting an increased contribution of the more red-shifted P_{D2} chromophore to the (P_{680}^{+}-P_{680}) difference spectrum. These observations were interpreted as indicating a dominant localization of the cation on P_{D1} with an increased sharing of the cation with P_{D2} under conditions which lowered the reduction potential of the latter (e.g. D2-His197Ala). Okubo et al. [50] have revisited the characterization of the intervalence band and the positions of the $C_{13}{}^{1}$=O keto stretch

in the P_{680}^{+}/P_{680} difference spectrum. They find the degree of delocalization to be limited in spinach PSII membranes and wild type *Thermosynechococcus elongatus* core complexes (70–80% localized) [50], in agreement with the conclusions drawn from ENDOR and from the optical characterization of the site-directed mutants. In contrast, FTIR measurements on D1D2-cytb_{559} reaction centers from spinach indicated the delocalization to be complete [50]. The increased localization of the P_{680}^{+} cation on P_{D1} compared to the purple bacterial reaction centers is likely to be a consequence of the slightly increased separation of the special pair chlorophylls resulting in a decreased overlap of the special pair wave functions [51]. One advantage of this increased localization is that it places the cation in closer proximity to redox-active tyrosine, Y_Z, the immediate secondary donor to P_{680}^{+}, accelerating the rate of electron transfer. As we will see below it also likely influences the reduction potential of the P_{680}^{+}/P_{680} redox couple.

3. Drawing the energetic picture of PSII from the kinetic studies

3.1. The various midpoint potentials usable as reference

Determining the free-energy level of the various states transiently formed during the turnover of Photosystem II is essential for the understanding of water-splitting because it puts severe constraints on the mechanistic models which can be considered. To date, only a limited number of electron carriers can be titrated and their midpoint potentials directly measured. Yet, these can serve as references and, provided the free-energy change associated with the electron transfer between one of these redox cofactors and another electron carrier is known, allow the determination of their relative reduction potentials. This strategy has been undertaken by many groups and a fairly complete picture emerges from these numerous studies. However, inconsistencies arise because different reference points are chosen. We will thus first discuss the various midpoint potentials that may be taken as references and, then, attempt to rebuild the entire energetic edifice of PSII. To date, the midpoint potential of four redox carriers has been directly determined by redox titration: $Pheo_{D1}$, Q_A, Y_D and cytochrome b_{559}. By measuring the amount of $Pheo^{-}$ which can be photo-accumulated, Klimov et al. [52] and Rutherford et al. [53] estimated the midpoint potential of the Pheo/$Pheo^{-}$ couple to be −600 to −650 mV, consistent with the more negative values reported in bacterial reaction centers which range from −400 to −600 mV [54–57]. Krieger et al. [58] nicely illustrated the range of factors that affect the measurement of the midpoint potentials. From a careful survey of the literature they collected 29 estimates ranging from −300 to +100 mV for the reduction potential of the Q_A/Q_A^{-} couple. A systematic evaluation of critical parameters such as the effects of redox mediators or the integrity of the Mn_4Ca cluster led these authors to favor −30 mV (in the presence of DCMU and with the cluster intact) as the most reliable value (see [58,59] for a discussion on the origin of the values in the −300 to +100 mV range). Another potential reference point is the midpoint potential of the Y_D^{ox}/Y_D couple which was measured at pH 8.4 in Mn-depleted PSII by Boussac and Etienne [60] who reported a value of 760 mV.

3.2. Does the difference in free-energy between the $P^{+}Pheo^{-}$ and $P^{+}Q_A^{-}$ states match the difference in redox potential of the $Pheo^{-}/Pheo$ and Q_A^{-}/Q_A couples?

Taking these various possible references as starting points, different strategies may be followed to infer the operating redox potentials of the other electron carriers. In each case, they rely on the determination of the free-energy change associated with a given electron transfer reaction and on the assumption that the difference in redox potential between the electron donor and acceptor is equal to this change. As just discussed, the redox potentials of the $Pheo_A/Pheo_A^{-}$ and Q_A/Q_A^{-} couples having been directly measured, one may evaluate this strategy by comparing the difference between these two ($\Delta E_{PheoQ} \sim -610$ mV) to the available estimates for the free-energy change associated with electron transfer between $Pheo_A$ and Q_A (ΔG_{PheoQ}). ΔG_{PheoQ} may be quantified by investigating the yield of the various recombination pathways involved in the decay of the $S_2Q_A^{-}$ charge separated state. Three routes should be considered which all involve the repopulation via Boltzmann equilibrium of the $P^{+}Q_A^{-}$ state. From this latter state, charge recombination may occur either via direct electron transfer between P^{+} and Q_A^{-} (direct pathway), or via the thermally activated repopulation of $P^{+}Pheo^{-}$ and the ensuing electron transfer between P^{+} and $Pheo^{-}$ (indirect pathway) or via the repopulation of the P^{*} state and the deactivation of this excited state (excitonic pathway). As first discussed by van Gorkom [61], the yield of the excitonic pathway would be much lower than experimentally found if ΔG_{PheoQ} were equal to ΔE_{PheoQ}. Indeed, the maximum rate for this pathway v_{exc} is k_{exc}/K_{exc}, where k_{exc} is the rate constant for exciton deactivation and K_{exc}, the equilibrium constant between $S_2Q_A^{-}$ and $S_1P^{*}Q_A$. Since the rate of charge recombination of the $S_2Q_A^{-}$ state is $\sim 0.2\ s^{-1}$ and $k_{exc} \approx 3.10^{8}\ s^{-1}$ [62,63], the finding of a 3% yield for the excitonic pathway [64] implies $v_{exc} \approx 0.2\ s^{-1} \times 0.03 = 6.10^{-3}\ s^{-1}$ and $K_{exc} \approx 5 \times 10^{10}$ which translates into a maximum of 640 meV for the free-energy gap between $S_2Q_A^{-}$ and $S_1P^{*}Q_A$. This mere finding shows that ΔG_{PheoQ} must be significantly smaller than ΔE_{PheoQ} since otherwise the remaining driving force for the formation of the $S_2Q_A^{-}$ state from $S_1P^{+}Q_A^{-}$ would be shockingly small (640–610 = 30 meV).

3.3. Operating versus midpoint potentials

Apparent contradictions between ΔG and ΔE_m are far from being unique to Photosystem II and have led to the distinction between 'equilibrium redox potential' and 'operating redox potential'. These differences arise because the two methods do not probe the same state of the redox cofactors. Two types of phenomena may account for these differences. One comes from the different time-domains involved in equilibrium redox titration and functional analysis. Whereas redox titrations require thermodynamic equilibrium between the sample and the solution

poised at a given electrochemical potential, the functional analysis allows one to probe transient states whose free-energy may differ significantly from that of the equilibrated states. Indeed, in response to the change in the redox state of a given cofactor, the protein environment may undergo energetic relaxation (such as proton transfer, conformational changes) which may be slower than the lifetime of the transient oxidized (or reduced) cofactor. Armstrong and colleagues have nicely illustrated this point with the 'fast-scan electrovoltammetric' technique [65]. Other examples are found in photosynthetic reaction centers (RC) (see, e.g. [66,67]). An alternative but non-exclusive explanation of the different E_ms yielded by redox titration and functional analysis relies on the fact that most of the membrane proteins involved in electron transfer reactions bind several cofactors which are usually located at less than 15 Å from one another. Such short distances may result in significant electrostatic interactions between the different cofactors. Thus, the free-energy level of a given cofactor includes the electrostatic contributions of the nearby electron carriers. Such a contribution has been nicely illustrated in the case of the tetraheme cytochrome of *Blastochloris* (formerly *Rhodopseudomonas*) *viridis* [68–70]. It is noteworthy, however, that throughout a redox titration, all of the cofactors undergo an identical charge change in terms of sign (i.e. all are either reduced or oxidized), whereas in an electron transfer chain, two nearby cofactors involved in an electron transfer reaction will undergo charge changes of opposite sign (one will be oxidized at the expense of the other). Consequently, if the electrostatic interaction between the two is significant, the difference between their equilibrium E_ms will be greater than the free-energy change associated with the electron transfer between them.

4. Energetics of the secondary and tertiary electron/proton transfer

4.1. Free-energy difference between P^+Pheo^- and $P^+Q_A^-$

Such electrostatic contributions may have significance with regard to the present issue of the apparent discrepancy between ΔG_{PheoQ} and ΔE_{PheoQ}. A first effect is the interaction between Pheo and the anionic quinone Q_A^- which might be present at the low potential poise where $Pheo_{D1}$ titrates (unless the doubly reduced Q_AH_2 is formed). Such interaction was estimated at 90 mV [71]. The second and presumably even more significant effect is the interaction between the cationic P^+ and $Pheo^-$ that should be taken into account when estimating the free-energy level of the P^+Pheo^- state but does not contribute to the equilibrium redox potential of the Pheo/$Pheo^-$ couple. From electrostatic calculations, Parson et al. [72] estimated this interaction between P^+ and $Pheo^-$ at 160 mV in the bacterial reaction centers, and Ishikita et al. [21] at 82 mV in PSII. Together with the 90 mV interaction with Q_A^- this would decrease ΔG_{PheoQ} with respect to ΔE_{PheoQ} by 170–250 meV so that ΔG_{PheoQ} would be ~440–360 meV. It should be noted that these two contributions mostly affect the free-energy level of the P^+Pheo^- state with respect to its expected value derived from the E_m of the Pheo/$Pheo^-$ couple, making the midpoint potential of the Q_A/Q_A^- couple a much more robust reference value (see Fig. 3). Based on this reference, one may then derive the operating redox potentials of the P^+/P and P^+/P^* couples.

4.2. Free-energy difference between S_1P^* and $S_2Q_A^-$

As described above, the free-energy gaps between $S_2Q_A^-$ and $S_1P^*Q_A$ on the one hand and $S_2Pheo^-Q_A$ on the other hand may be estimated from the combined knowledge of the respective deactivation rates and yields of the different charge recombination pathways. The yield of the indirect pathway has been estimated by comparing the lifetime of the $S_2Q_A^-$ state in Photosystem II mutants of *Synechocystis* 6803 bearing site-directed replacements of the D_1-Gln130 residue [17,18] which is involved in a H-bond with the $C_{13}{}^1$=O of $Pheo_A$ [15]. The strength of the H-bond is expected to modify the redox potential of the Pheo/$Pheo^-$ couple (the stronger the H-bond the more positive the redox potential) and hence the yield of the indirect pathway. Accordingly, the recombination rate of the $S_2Q_A^-$ state was found to increase with the H-bond strength [19,73,74], arguing for the significance of the indirect pathway in the overall charge recombination process. This point was further supported by changes in the thermoluminescence band intensity resulting from mutation-induced modifications of the free-energy level of the P^+Pheo^- state, demonstrating, as previously proposed by van Gorkom [61] and Vavilin and Vermaas [75] that the excitonic pathway is by-passed by the indirect pathway [19,76]. In addition to this qualitative agreement, the comparison of the $S_2Q_A^-$ lifetime in the various mutants allowed the estimation of the intrinsic rates of the various pathways (and hence of their respective yields) either by relying on the published estimates [18] for the changes in the free-energy level of the P^+Pheo^- state [73] or on the direct quantification of these changes through the mutation-induced modification of the thermoluminescence band intensity [19]. Both approaches yielded similar values: Rappaport et al. [73] estimated the rate and yield of the direct pathway at $v_{dir} = 0.05\,s^{-1}$ and $\Phi_{dir} = 23\%$ (or $v_{ind} \approx 0.17\,s^{-1}$), respectively, and Cser and Vass [19] found $v_{dir} = 0.09\,s^{-1}$ and $\Phi_{dir} = 12\%$ (or $v_{ind} \approx 0.67\,s^{-1}$). As described in [73] $v_{ind} = k'_{PhQ}/K_{SP}K_{PhQ}$ with $k'_{PhQ} = k_{PhQ}k_{PhP}/k_{PhQ} + k_{PhP}$ where K_{SP} and K_{PhQ} stand for the equilibrium between S_2P and S_1P^+ and between $P^+Q_A^-$ and P^+Pheo^-, respectively, and k_{PhQ} and k_{PhP} stand for the electron transfer rates between $Pheo^-$ and Q_A and $Pheo^-$ and P^+, respectively. As these two latter values are known from the literature ($k_{PhQ} = 3.3 \times 10^9\,s^{-1}$ [77–80] and $k_{PhP} = 3 \times 10^9\,s^{-1}$ [81]), the free-energy gap between $S_2Q_A^-$ and P^+Pheo^- can be estimated to be 560–590 meV (see Figs. 2 and 3). Interestingly enough, these studies also allow one to assess the free-energy gap between the $S_2Q_A^-$ and $P^+Q_A^-$ states and thus to extract ΔG_{PheoQ} from the above value. Indeed, the rate of decay of the $S_2Q_A^-$ state via the direct pathway (v_{dir}) may be compared to the electron tunneling rate between P^+ and Q_A^- (k_{PQ}) and yield K_{SP}. The rate of $P^+Q_A^-$ decay at cryogenic temperatures (which blocks the indirect and excitonic pathways) was reported to be $410\,s^{-1}$ [82,83]. This is similar to the

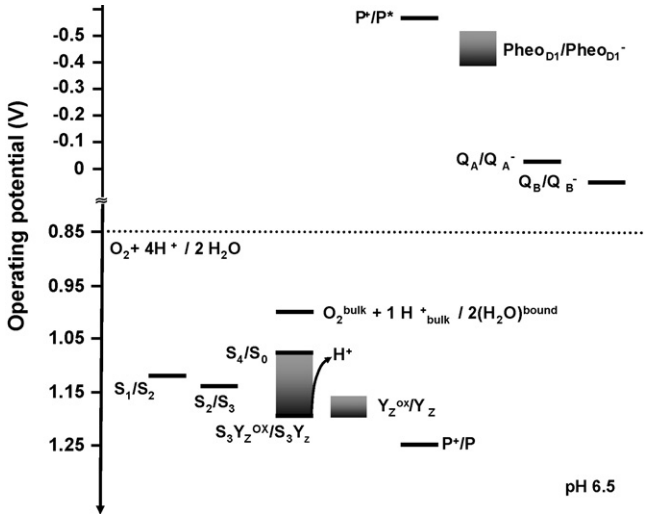

Fig. 3. The operating potentials of the essential redox components in Photosystem II when the midpoint potential of the Q_A/Q_A^- couple (−30 mV, [58]) is taken as a reference. Note that, as discussed in the text, these operating potentials are determined on the basis of the experimentally accessible free energy changes associated with the different electron transfer steps. The time-dependent relaxation processes are indicated by shaded boxes.

expected tunneling rate derived from Marcus theory (500 s^{-1}, [83]) and since $K_{SP} = k_{PQ}/v_{dir} \approx 5500 - 8200$, one obtains $\Delta G_{SP} \approx 220$–240 meV and $\Delta G_{PheoQ} \approx 320$–370 meV [73]. De Wijn and van Gorkom [84] reached a similar estimate to account for the low yield of the direct charge recombination pathway with respect to the indirect non-radiative one. From ps-luminescence decay measurements, the free-energy change associated with the exciton trapping has been estimated by various groups using different materials. Here again, a fairly consistent pictures emerges. Using D_1D_2-b_{559} reaction centers, Booth et al. [85] found that the free-energy difference between P^* and P^+Pheo^- was ∼135 meV. When using PSII particles, the free-energy change associated with exciton trapping was ∼45 meV and the energy difference between P^* and the radical pair was ∼165 meV [71,86,87], yielding an entropic stabilization due to the dilution of the exciton over the antenna of ∼120 meV. In the case of intact PSII, with an antenna containing ∼200 Chls, this stabilization should be slightly larger and accounts for an energy difference of 140 meV between P^* and the exciton, yielding ∼185 meV between P^* and the radical pair. Reassuringly, addition of the 45 meV resulting from charge separation to the 560–590 meV difference between $S_2Q_A^-$ and P^+Pheo^- yields a free-energy gap between the exciton and $S_2Q_A^-$ of 605–635 meV, a figure which closely matches the 640 meV estimated by van Gorkom and co-workers from the yield of the excitonic pathway. The reasonable agreement between various approaches taken by different groups places P^* 750–780 meV above $S_2Q_A^-$. Recently, Grabolle and Dau revisited these issues with a different approach from those just discussed which mostly relied on the kinetic analysis of the charge recombination process. By a careful calibration of the delayed fluorescence yield based on the measure of the prompt fluorescence yield, they could quantify the fraction of PSII in the excited state in Boltzmann equilibrium with the charge separated state, and directly infer the free-energy difference between the considered states. A value of 430 meV was found for the energy difference between $Y_Z^{ox}Q_A^-$ and the exciton, which after substraction of the 38 meV associated with reduction of P^+ by Y_Z in the time-range studied and of the 45 meV associated with exciton trapping leads to ∼345 meV between P^+Pheo^- and $P^+Q_A^-$ [88].

4.3. The operating potential of P_{680}^+/P_{680}

From this non-exhaustive survey of the literature, it appears that, electroluminescence, thermoluminescence, kinetic studies of charge recombination or delayed fluorescence have led to rather similar figures so that one can start to draw with reasonable confidence the energetic picture of PSII. The free-energy difference of 500 meV [88] or 540 meV [73] between P^* and $P^+Q_A^-$ is particularly interesting as, with the midpoint potential of the Q_A/Q_A^- couple as a reference (−30 mV in the presence of DCMU [58]), it yields an estimate of the absolute midpoint potential of the P^+/P^* redox couple and hence of the P^+/P couple after the addition of the energy of the singlet-singlet transition of P: E_m (P^+/P) ∼−570 + 1830 ≈ 1250 mV. Since, as discussed above, the cation mostly resides on the P_{D1} chlorophyll, this value may be compared with the midpoint potential obtained by solving the Poisson–Boltzmann equation for PSII: 1.25 V [22]. It should be stressed that, given the uncertainties of the various figures used in the preceding estimation of E_m (P_{680}^+/P_{680}), the perfect numerical agreement is likely to be coincidental although it certainly brings support to the entire edifice.

4.4. Factors that modulate the reduction potential of the primary donor

The need for an elevated reduction potential for P_{680}^+/P_{680} is critical to the requirement of the reaction center to be able to drive the oxidation of water to molecular oxygen, a process that requires a reduction potential of ≥0.9 V at pH 6, the estimated pH of the lumenal space of the thylakoid at modest photon fluxes [89]. Certainly, a major contributor to the elevated reduction potential of P_{680}^+/P_{680} over P_{870}^+/P_{870} is the replacement of Bchlorophyll a with chlorophyll a the midpoint potentials of which differ by 160 mV in CH_2Cl. This difference is in large part due to the stabilization of the HOMO in Chl by its more extensive π-system relative to Bchl [90]. There must, however, be other factors in play as the reduction potentials of the redox couples P_{680}^+/P_{680} and P_{700}^+/P_{700} differ by ∼800 mV despite the fact that both are weakly coupled chlorophyll dimers. A consequence of the increased localization of the P_{680}^+ cation mentioned above is that it is likely to increase the reduction potential of the P_{680}^+/P_{680} redox couple over what it would be in the delocalized state [51,91]. An example of the influence of charge localization between the special pair BChls on the reduction potential of the primary donor has been demonstrated in *Rb. sphaeroides* reaction centers where in the wild-type the cation is delocalized favoring the P_L over P_M by a factor of 2:1 [92] to 3:1. Ivancich et al. [93] have analyzed a series of eight site-directed mutations at M160 which increase the strength of the hydrogen bond to the C_{13}^1=O carbonyl of the P_M BChl.

The hydrogen bond is proposed to stabilize the P_M HOMO and that of the special pair dimer, raising the reduction potential of the P_{870}^+/P_{870} redox couple. A correlation was demonstrated between increased localization of the cationic charge on P_L and an increase in the P_{870}^+/P_{870} reduction potential. A more extreme example involves the replacement of M-His202, the axial ligand to P_M, with Leu which results in the replacement of the M side special pair BChl with a BPhe, producing complete localization of the cation on P_L [94,95] and an increase in the reduction potential of P_{870}^+/P_{870} from 505 ± 5 to 640 ± 10 mV [94,96]. The influence of delocalization on the P_{680}^+/P_{680} reduction potential has been invoked by Okubo et al. [50] as a possible reason for why P_{680}^+ is unable to oxidize Y_Z in D_1D_2-cytb_{559} reaction centers where the cation is completely delocalized.

Allen et al. [96] have manipulated two sets of hydrogen bonds to P_L in the M-His202Leu *Rb. sphaeroides* heterodimer mutant, where the cationic charge is already localized on P_L. The mutation L-Leu131His introduces a hydrogen bond between histidine and the $C_{13}{}^1$=O carbonyl of the BChl P_L whereas L-His168Phe removes a hydrogen bond to the C_2-acetyl group of the BChl P_L. The former raises the midpoint potential of P^+/P by 80 mV while the latter decreases the midpoint potential of P^+/P by 85 mV. Mutations that introduce hydrogen bonds to the BPheo of the heterodimer have much smaller effects on the Em of P^+/P (+15 mV) consistent with the localization of the cationic charge on P_L in the heterodimer. Clearly, the hydrogen bonds increase the reduction potential of the Bchl to which they are introduced. In the case of PSII, however, the hydrogen bonds to the $C_{13}{}^1$=O carbonyls of both P_{D1} and P_{D2} are thought to be quite weak from FTIR [46,50,97–99] with C=O stretching frequencies of $\sim$1700 cm^{-1}. This prediction has been borne out by the X-ray crystal structure which indicates the absence of a hydrogen bonding residue [8,13,23], implying that such hydrogen bonding is not a major factor in the elevated reduction potential of P^+/P. There is, however, a likely hydrogen bond to the $C_{13}{}^1$=O of Chl_{D1} (FTIR stretch 1669 cm^{-1}) [46], not visible in the PSII X-ray structures, but likely provided by a bridging water molecule from D2-His197, by analogy with purple bacterial reaction centers [100]. This hydrogen bond likely contributes to raising the reduction potential of the Chl_{D1}^+/Chl_{D1} redox couple relative to P^+/P. Indeed, site-directed mutations that weaken the hydrogen bond appear to accelerate the rate of $S_2Q_A^-$ charge recombination, presumably by lowering the reduction potential of the Chl_{D1}^+/Chl_{D1} redox couple (Rachel Cohen, unpublished results).

Another factor that contributes to the tuning of the chlorophyll reduction potential is the distortion of the tetrapyrrole head group, which decreases the extent of conjugation, raising the HOMO and decreasing the reduction potential. Such distortion has been noted in the Chla of P_{700} in PSI [40,90]. The reduction potential of P_{680}^+/P_{680} would be maximized by making the tetrapyrrole head group of P_{D1} as planar as possible, coplanarity of the $C_{13}{}^1$=O in ring V which would likely maximize the electron withdrawing properties of this substituent and coplanarity of the vinyl group which would extend the π-system [40,90].

Charges are also likely to exert considerable influence over redox tuning, with plus charges raising the P^+/P reduction potential and negative charges doing the opposite. Such charges have been considered in detail by Ishikata et al. [91], who have compared the X-ray structures of PSII and PSI and attribute the upshift of the reduction potential of P_{680}^+/P_{680} relative to that of P_{700}^+/P_{700} to the following factors: 1) atomic charges associated with the peripheral subunits (upshifting the Em of P_{680}^+/P_{680} by 170–200 mV relative to P_{700}^+/P_{700}); 2) the positions of axial ligands to P_{D1} and P_{D2} at the lumenal end of the transmembrane D-helix as opposed to their location 8 residues from the end in the transmembrane J-helix in the case of P_A and P_B of PSI. The location of the pigments relative to the protein helical dipoles result in an overall upshift of the Em of P_{680}^+/P_{680} by 130–140 mV relative to the E_m upshift of $\sim$30 mV for P_{700}^+/P_{700}; and 3) the charges associated with the Mn_4Ca cluster (upshifting the E_m of P_{D1} and P_{D2} by 210 and 110 mV, respectively). As far as this latter contribution is concerned, experimental data are suggestive, however, that removing the Mn_4Ca cluster rather results in an increase of the equibrium constant between $P_{680}{}^+Y_Z$ and $P_{680}Y_Z{}^{ox}$ (see below) at odds with the expected downshift in the E_m of P_{680}^+/P_{680} resulting from the disassembly of the cluster.

Another factor that affects the reduction potential of P_{680}^+/P_{680} is the axial coordination of chlorophyll. Site-directed mutations were constructed in *Synechocystis* 6803 at D1-His198 and D2-His197, replacing the axial ligands to P_{D1} and P_{D2} with a wide range of residues. Some of these were characterized kinetically to determine the extent of radical pair formation [18] and the apparent equilibrium constant for the reaction $Y_ZP_{680}{}^+ = Y_Z{}^\bullet(H^+)P_{680}$ [32,101]. Replacement of D1-His198 with Gln and Lys produced increases in the P_{680}^+/P_{680} reduction potential (0–53 and 88 mV, respectively) while Ala, Cys, Glu and Ser produced substantial decreases (-29 to -82 mV; -77; -117; and -112 mV, respectively) ([32] and see also [19]). The increase in the His to Gln and His to Lys mutants likely results from the loss of the polarizable His coordination and its replacement with a cationic residue, respectively. Cys and Glu provide anionic ligands while the Ala and Ser replacements most likely result in axial coordination by a water molecule which deprotonates upon formation of $P_{D1}{}^+$. In all of these four cases, an anionic ligand stabilizes the cation, lowering the reduction potential. Replacements of D1-His198 with Leu [32] and D2-His198 with Leu [32] and Tyr [102] resulted in no stable accumulation of reaction centers, presumably because they interfere sterically with the coordination of a chlorophyll, preventing proper folding of the polypeptide. It was thus not possible to construct a heterodimeric special pair in PSII as in the case of the bacterial reaction centers (see above).

4.5. The operating potential of $Y_Z{}^{ox}/Y_Z$

The combined knowledge of the free-energy changes associated with Y_Z oxidation on the one hand and of the redox potential of the P_{680}^+/P_{680} couple, on the other hand, sets the operating redox potential of the Y^{ox}/Y_Z couple. Yet, as will be discussed below, proton release may occur, depending on the S-states, in a time-range similar to the lifetime of $Y_Z{}^{ox}$. As a proton transfer is associated with significant relaxation energy, the operating midpoint potential of Y_Z ought to be defined as

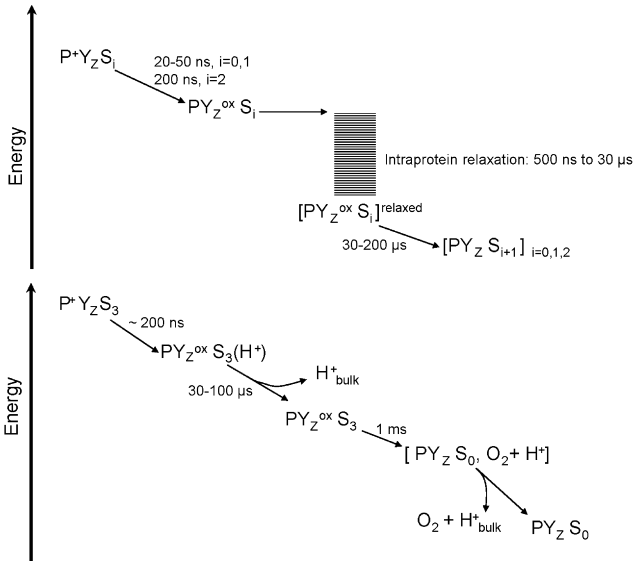

Fig. 4. Electron transfer and proton transfer dynamics in Photosystem II: the electron donor side. The top panel applies to the S_0 to S_1, S_1 to S_2 and S_2 to S_3 transitions whereas the bottom panel is a focus on the S_3 to S_0 transition. See text for a detailed discussion.

a function of time (see Fig. 4). In O_2-evolving PSII, the free-energy change associated with Y_Z oxidation has been inferred from the rate of reduction of P^+. These kinetics are strongly multiphasic (see [103–106] for reviews). By studying the consequences of H/D substitution, various groups have proposed that the fast phases (sub-μs) correspond to pure electron transfer steps whereas the slow phases, apparent in the μs to tens of μs time-range reflect relaxation processes likely resulting from proton transfer ([107–110,104,106] for reviews). In an attempt to discriminate the energetics of these various processes, we will define the operating midpoint potential of Y_Z^{ox} at 2 μs, a time which is long enough to allow completion of the electron transfer steps but not of the ensuing relaxation steps. Furthermore, as the equilibrium between $P_{680}^+Y_Z$ and $P_{680}Y_Z^{ox}$ depends on the S-states, we will focus on the value of the equilibrium constant in the presence of the S_3 state. There is a general agreement that the free-energy drop associated with Y_Z oxidation is small, 20–40 meV [103,111,112]; so that the operating midpoint potential of the Y_Z^{ox}/Y_Z couple would be ∼1.2 V (see Figs. 3 and 4).

4.6. The operating potentials of the S_i/S_{i+1} couples

The equilibrium constants between $Y_Z^{ox}S_i$ and Y_ZS_{i+1} were determined by electroluminescence studies and were found to be dependent on the S-states: 9 (55 meV), 5 (40 meV) and 65, (105 meV) for the S_1, S_2 and S_3 states at pH 6.6, respectively [113] (see Fig. 3). It should be noted, that the amplitudes of electroluminescence were measured 20 μs after the flash so that, as alluded to above, relaxation processes leading to the stabilization of Y_Z^{ox} should be taken into account. These were estimated to be ∼20 meV by Jeans et al. [112]. Altogether this would locate the midpoint potentials of the S_1/S_2, S_2/S_3 and S_3/S_0 couple in the 1.12, 1.14 and 1.08 V range, respectively. The free-energy gap between $P_{680}^+S_1$ and $P_{680}S_2$ would thus be ∼130 meV which is about 110 meV smaller than the estimate of 240 meV obtained above from the analysis of the kinetics of charge recombination. The discrepancy, between the charge recombination analysis and the electroluminescence studies may however be smaller since the latter approach probed the stabilization in energy provided by the successive forward electron transfer/proton transfer steps, whereas the former probed the decay of the relaxed charge separated state to the ground state. Consistent with this, Vos et al. observed luminescence decay occurring in the 15–400 ms time-range (i.e. slower than Y_Z^{ox} reduction by the S-states) that were ascribed to relaxation processes. These components provide an additional stabilization by a factor of 6 to the S_2 state, which translates, into an additional drop in free-energy by ∼50 meV [113]. Considering the uncertainties of the various values which need to be added and the different experimental conditions, such as pH, the agreement between the different approaches described here is, in our opinion, satisfying.

4.7. Can the midpoint potential of Y_D^{ox}/Y_D serve as a reference?

Until now we have mostly relied on the midpoint potential of the Q_A/Q_A^- couple as a reference. Although we discussed the reason which led us to dismiss the midpoint potential of the Pheo/Pheo$^-$ couple, the robustness of the above described energetic construct should be evaluated in comparison with other reference points. The midpoint potential of the Y_D^{ox}/Y_D has been titrated in Mn-depleted PSII at pH 8.5 by Boussac and Etienne who determined a value of 760 mV [60]. By studying the rate of reduction of Y_D^{ox} by phenylenediamine, interpreted as occurring via the reduction of Y_Z^{ox} and the equilibrium $Y_ZY_D^{ox} \leftrightarrow Y_Z^{ox}Y_D$ equilibrium, they estimated the free-energy gap between these two states at 240 meV [114]. This would place the $E_m(Y_Z)$, in Mn-depleted PSII, at 1 V, i.e. about 200 mV below the above estimates. There is general agreement that the equilibrium constant for electron transfer between Y_Z and P_{680}^+ is significantly larger in Mn-depleted PSII than in the presence of the Mn_4Ca cluster. Besides the possible structural changes, resulting from the disassembly of the cluster, this difference likely stems from the fact that in the absence of the Mn_4Ca cluster Y_Z is the terminal electron donor so that the estimated equilibrium constants deal with the relaxed states. Comparing the rates of charge recombination of the $Y_Z^{ox}Q_A^-$ and $P_{680}^+Q_A^-$ states has led to estimates for the free-energy between these two of 160–210 meV at basic pH [111,115–117] so that, when taking 1.25 V as a reference for the P_{680}^+/P_{680} couple, the redox potential of the Y_Z^{ox}/Y_Z couple would be ∼1.05 V in reasonable agreement with the estimate derived by Boussac and Etienne [60]. The use of the latter estimate requires some caution as the EPR spectrum for Y_D^{ox}, on which the titration was based, is lacking in hyperfine structure and there may have been some chemical modification induced by the use of the strong oxidant K_2IrCl_6. Another possible difficulty with the use of the midpoint potential of Y_D^{ox}/Y_D as a reference is its likely but, to our knowledge, yet uncharacterized dependence upon pH. Indeed recent studies have shown that the rate of oxidation of Y_D is strongly dependent upon pH, slowing dramatically below pH 7.7 ([118]

and [119] for a review). This observation was interpreted as reflecting the protonation of a residue which would otherwise have served as a proton acceptor in the phenolic proton transfer which would normally accompany the oxidation of Y_D. As ENDOR [120] and FTIR [98] studies have shown that Y_D^{ox} is a neutral radical, the phenolic proton released upon its formation was proposed to be borne at least partially by D_2-His189 [118,121], the source of the hydrogen bond to Y_D^{ox} (see [122]). In any case, were a positive charge to be trapped in the vicinity of Y_D^{ox} at pH 7.7, it would significantly raise the Y_D^{ox}/Y_D midpoint potential. But is it trapped? In addition to the pH effect on the yield of Y_D oxidation, evidence that the proton released upon Y_D oxidation is indeed retained in its vicinity comes from an electrochromic shift of P_{D2} when Y_D is oxidized [32,123]. Furthermore, light-induced assembly of the Mn cluster is less efficient in a mutant lacking Y_D, consistent with the implicit hypothesis that the presence Y_D^{ox} modifies the energetic picture in PSII [124]. Yet, the various studies aimed at quantifying the electrostatic consequences of the positive charge associated with Y_D^{ox} by comparing the kinetics of reduction of P_{680}^+ or the (P_{680}^+-P) difference spectrum in a WT (with Y_D oxidized) and a mutant lacking Y_D consistently pointed to surprisingly small differences [101,125,126]. As discussed in [101,119] this apparent lack of electrostatic effect of Y_D^{ox} may merely result from the fact that at low pH, the proton acceptor is protonated in the mutant and would mimic the formation of $Y_D^{\bullet}(H^+)$ in the WT. At pH 6.0, Vass and Styring estimated the free-energy gap between $Y_D^{ox}S_1$ and Y_DS_2 to be ~170 meV [127] by comparing the lifetime of the $Y_D^{ox}S_1$ to the rate of deactivation of state S_2 to S_1. Taking the value of 1 V determined above for the S_2/S_1 couple (we take the "relaxed" value since the decay of $Y_D^{ox}S_1$ has a 500 min half-time), places the midpoint potential of Y_D^{ox}/Y_D at 830 mV at pH 6.0, i.e. only 70 mV above the 760 mV obtained at pH 8.5, an increase which is far from unrealistic considering the 150 meV that could provide the 2.5 pH unit difference in pH. It should be noticed, however, that the lifetime of $Y_D^{ox}S_1$ is smaller at pH 8.5 than 6.5 suggesting that the equilibrium with Y_DS_2 is shallower at high pH [127]. Yet, the oxygen evolution capacity of PSII decreases as the pH increases so that the integrity of the Mn_4Ca cluster may be questioned at pH 8.5. Furthermore, as emphasized by the authors [127], given the lifetime of the $Y_D^{ox}S_1$ state (hundreds of minutes), other processes may compete with the considered pathway involving equilibrium with the S_2Y_D state and the deactivation of S_2 into S_1 so that comparing the lifetime of the $Y_D^{ox}S_1$ and S_2 states only yields a lower limit for the redox potential difference. Altogether, the redox potential of the Y_D^{ox}/Y_D couple determined at pH 8.5 in Mn-depleted PSII is probably not a reliable base upon which to construct the energetics of oxygen-evolving PSII.

5. The energetics of water-splitting

5.1. Is water-splitting driven by entropy changes?

There is, however, another available redox couple which, at first sight, should be an inescapable reference: the redox potential of the $O_2/2H_2O$ couple. Obviously, from the outcome of the oxygen evolving complex turnover: $S_4 + 2H_2O \leftrightarrow S_0 + O_2 + 4H^+$, it follows that, were the reaction occurring in solution, its equilibrium constant would be the difference between the redox potential of the $S_3Y_Z^{ox}/S_0$ and $O_2/2H_2O$ couples. In this case, the redox potential of the latter couple, 815 mV at pH 7, would set the lower limit for the necessary oxidizing potential. Yet, because the free-energy difference includes purely entropic terms, such as dilution of the product ($4H^+$ and O_2), the relevant free-energy difference of the elementary water-splitting reaction at the level of the catalytic site is expected to be significantly smaller, a point that was strongly made by Krishtalik [128,129]. This led him to introduce the concept of the 'configurational potential', E_c, which is obtained from the standard potential after subtraction of the terms depending on the concentration of the reactant and products [128]. In the likely case where splitting of $2H_2O$ molecules follows an overall four electron reaction, E_c was estimated at 1.4 V. This is significantly higher than the available oxidizing power discussed above, which would suggest that water-splitting *per se* is a strongly activated process, mostly driven by the increase in entropy resulting from the dilution of the products. Yet, the value of 1.4 V is most likely overestimated. As discussed in detail by Krishtalik, several factors may concur to decrease the activation energy of the elementary steps. Prominent among them is the presence of a proton-accepting group, which would be deprotonated beforehand during the steps preceding water-splitting [128]. By acting as a strong base during the water-splitting process, it would decrease the number of released H^+ and hence the difference between the standard and configurational potentials of the $O_2/2H_2O$ couple. This points to the issue of the stoichiometry of proton release accompanying the $S_4 + 2H_2O \leftrightarrow S_0 + O_2$. Although, this has been a strongly debated issue, it is now agreed that the overall S_3 to S_0 step leads to the release of ~$2H^+$ (see [130] for a review and [131–134]). Furthermore, based on the time-resolved measurement of the electrochromic band-shift associated with Y_Z^{ox} [135], of the proton release [133] or of delayed luminescence [136], proton release has been proposed to occur upon formation of the $Y_Z^{ox}S_3$ state and prior to the reduction of Y_Z^{ox} (see Fig. 4). As a consequence, about three weak acids would be deprotonated before S_4 is formed and may act as strong bases and bind the product H^+ as their pK_as are reset when electrons are abstracted from water. These bases would further facilitate water oxidation, i.e. decrease the activation energy of the elementary steps, by promoting deprotonation of the substrate; the free-energy change resulting from this proton transfer being proportional to the difference between the pK_as of the proton acceptor and donor (H_2O) (see the review by H. Dau and M. Haumann in this issue for a more detailed discussion). That such processes are indeed at work in PSII was experimentally substantiated by the observation that the overall $S_4 \rightarrow S_0 + O_2$ step, which develops with a 1.2 ms half-time, was preceded by an electrostatic relaxation phase [135,136]. By following the reduction of Y_Z, at 295 nm, Rappaport et al. showed that electron transfer to the $S_3Y_Z^{ox}$ state was preceded by a lag phase with a 30 μs half-time. This lag phase in the electron transfer sequence was accompanied by a decrease in the amplitude of the electrochromic band-shift associated with the formation of

the $S_3Y_Z^{ox}$ state. It was therefore proposed that, in the presence of S_3, the formation of Y_Z^{ox} triggers the expulsion of a proton from a yet unidentified group, thereby allowing the splitting of water into dioxygen to take place [135]. The existence of this lag phase was confirmed by time-resolved EPR studies of the decay of $S_3Y_Z^{ox}$ [137]. Haumann et al. have recently provided elegant support for this model by using time-resolved X-ray absorption spectroscopy to directly follow the redox changes of the Mn_4Ca cluster [136]. By carefully choosing a wavelength specific to the S_3 to S_0 transition, they unambiguously resolve a lag phase of 200 μs duration in the reduction of the Mn_4Ca cluster (we note that the half-time of 30 μs determined earlier by Rappaport et al. translates into an approximate duration of 150–200 μs for the lag phase). Furthermore, this lag phase was shown to be accompanied by a decay of the delayed fluorescence yield developing in the hundred μs time-range. The temperature dependence of the amplitude of this decay indicates that it is entropy driven, as expected for a proton release step [136]. Interestingly, the change in free-energy associated with the proton release step was found to be only slightly pH dependent (80 meV at pH 5.2 and 110 meV at pH 6.4, see supporting online material in [136]) suggesting that equilibrium with the bulk is not achieved when electron transfer takes place, or, in other words, that part of the driving force made available for proton expulsion is in fact kinetically trapped and utilized to drive water oxidation.

5.2. Reversing water-splitting by O_2 backpressure

The fact that water-splitting is, at least partly, driven by the entropic contribution resulting from the dilution of the products has been recently illustrated by the impressive work of Clausen and Junge who showed that water-splitting can be driven backwards by increasing the O_2 pressure [138–140]. This observation, in addition to the research field it opens by providing means to force the accumulation of reaction intermediates on the way to oxygen formation, raises important energetic issues. It unambiguously shows that the overall driving force for water-splitting is relatively weak since a 10-fold increase in O_2 pressure turned out to be sufficient to half-suppress oxygen evolution. Moreover, by using the amplitude of the 1 ms phase (monitored either in the UV or through delayed fluorescence yield) as a signature of the advancement of the reaction toward O_2 production and plotting its amplitude as a function of O_2 pressure, they could estimate the overall driving force of the reaction to ∼−80 meV, at pH 6.7 [138,139], a figure which is close to the −105 meV reported in [113]. It should be noted that the free-energy difference derived from these experiments relates to the oxidation of the two water substrate molecules by the $S_3Y_Z^{ox}(S_4)$ state together with the release of the product into the bulk. It thus does not include the energy terms corresponding to the binding of the two water molecules to the catalytic site and their activation as substrate, and this could, at least partly, account for the fact that it is significantly smaller than the difference in midpoint potential of the $O_2/2H_2O$ (∼850 mV, at pH 6.5) and S_4/S_0 (∼1.1 V see above) couples. Consistent with this, O^{18} exchange studies showed that the affinity for the second water molecule increases 5-fold upon formation of S_3 [141] and led to the proposal that the entry of the second substrate water molecule into the catalytic site and the optimization of the positioning of the reactants would only occur after S_3 is formed [142,143]. Another important outcome of the experiments of Clausen and Junge is the finding that the amplitude of the 1 ms phase, associated with the decay of $S_3Y_Z^{ox}$, decreases as the O_2 pressure is increased. This observation puts strong constraints on the energetic profile of the successive steps which are likely to occur along the process of water-splitting. If one considers a sequence of elementary reactions: $A_0 \leftrightarrow A_1 \leftrightarrow A_2 \leftrightarrow \ldots \leftrightarrow A_n$, raising the free-energy level of the last state in the chain, A_n, is expected to decrease the overall free-energy gap between A_0 and A_n and hence the advance of the overall reaction, as depicted in [138,139]. Yet, it does not necessarily imply that the equilibrium population of A_0 should significantly increase. Indeed, if one of the various intermediates, A_i for example, lies well below A_0 in energy, decreasing $\Delta G_{A(n-1)An}$ and thus ΔG_{A0An} will mostly increase the probability for finding A_i, rather than A_0. The UV measurements may be ambiguous in this respect because an absorbance change remaining under high O_2 pressure could attest to the accumulation of any of the A_i's provided it absorbs in this wavelength region. However, the delayed fluorescence measurements clearly indicate that a high-energy state is trapped by the O_2 backpressure, so that one may conclude that the overall water-splitting reaction is unlikely to involve any step strongly downhill in energy (see Figs. 3 and 4).

5.3. Charge recombination and the phenomenological miss factor

The various thermodynamic and kinetic issues discussed so far are not only essential for the understanding of how water oxidation is energetically driven, but they also determine the yield of the overall process of energy conversion. Besides the efficiency of trapping and converting a photon into photochemical energy (the quantum yield), the losses of the system are experimentally observed by the damped oscillations of the flash-induced oxygen yields in a series of saturating flashes [1,2]. This damping was accounted for by incorporating in the S-state cycle a miss factor, a statistical probability that a PSII fails to increment the S-states after a saturating flash. Two non-exclusive possibilities can account for such misses. The photochemical trap may either be inactive when hit by a photon, or alternatively act as a trap but be inefficient in stabilizing the charge separated state. The first case has been extensively treated by Shinkarev and Wraight [144,145] who attributed the probability of misses to that fraction of PSII that is in the $P_{680}{}^+Q_A$ or $P_{680}Q_A{}^-$ states, or in other terms, on the equilibria at the donor and acceptor sides of PSII. Whereas the relatively small equilibrium constant between $Q_A{}^-Q_B$ and $Q_AQ_B{}^-$ (∼20 at pH 7 [146,147]) indeed predicts that 5% of the centers should be closed when an even-numbered flash is fired (and thus 2.5% on the average), the equilibrium constants between $P_{680}{}^+S_i$ and $P_{680}S_{i+1}$ are too large (∼10^4, see above) for a significant fraction of centers to be in the $P_{680}{}^+$ state before any flash. As typical values for the miss factor are on the order of 10%, the probability for a photon to hit an inactive trap thus seems too low to account for the totality of the

misses. Thus, there must be PSII centers in which charge separation occurs without being stabilized by an increment of the S-states cycle. This issue was recently revisited by de Wijn and van Gorkom [84,148,149], who studied the decay of P_{680}^+ via time-dependent changes in the fluorescence yield or electroluminescence. They observed that ~5% of the misses are caused by $P_{680}^+Q_A^-$ charge recombination, suggesting that this process competes with the reduction of P_{680}^+ by Y_Z. Furthermore, the probability for such a loss was found to increase with the oxidation state of the Mn_4Ca complex, with half of it occurring in the presence of S_3 [148]. This observation is consistent with the features discussed above for the thermodynamic and kinetic parameters associated with the reduction of P_{680}^+ since the low equilibrium constant between $P_{680}^+Y_Z$ and $P_{680}Y_Z^{ox}$ together with the relatively slow relaxation process result in a significant fraction of $P_{680}^+Q_A^-$ which has a long enough lifetime to undergo charge recombination. As pointed out in [104,149], the issue as to whether these relaxation phases reflect homogeneous (i.e. the probability for their occurrence in a given center is the same for all centers) or heterogeneous processes (different conformations which inter-convert in a longer time-domain than that of the studied process) is still unresolved. By comparing the misses in the period four oscillations of the electroluminescence burst arising from $P^+Q_A^-$ or $Y_Z^{ox}Q_A^-$, de Wijn and van Gorkom concluded that the population of active centers undergoing charge separation loss via either of these two processes is redistributed between flashes, placing an upper limit of tens of ms on the redistribution time [149]. Evidence for the existence of two slowly inter-converting populations of PSII reaction centers, with different efficiencies with respect to the stabilization of charge separation, comes from the finding that more than 10 ms is required after a saturating flash to convert the PSII reaction centers in which charge recombination has occurred into efficient stabilizers [150]. Although, there is presently no structural rationale for the existence, in a small fraction of centers (~5%), of a conformation that would be inefficient in the stabilization of charge separation, a heterogeneity in the H-bond network which likely participates in proton transfer associated with slow components in P_{680}^+ reduction, as initially proposed by Tommos and Babcock [151], is a good candidate. In addition to these intrinsic PSII properties, the efficiency of PSII to stabilize the charge separation when kept in its native environment (i.e. a coupled membrane) is expected to depend significantly on the transmembrane electrochemical potential, which builds up upon illumination of intact photosynthetic membranes. Indeed, the quantum yield on the one hand, and the probability for charge recombination on the other hand, have been shown to be, respectively, decreased and enhanced by a transmembrane electrochemical potential [152–156].

Acknowledgement

B.A.D. gratefully acknowledges financial support from National Research Initiative of the USDA Cooperative State Research, Education and Extension Service, grant number 2003-35318-13589.

References

[1] B. Kok, B. Forbush, M. McGloin, Photochem. Photobiol. 11 (1970) 457.
[2] P. Joliot, B. Kok, in: Govindjee (Ed.), Bioenergetics of Photosynthesis, Academic Press, New York, 1975, p. 387.
[3] B.A. Diner, F. Rappaport, Annu. Rev. Plant Biol. 53 (2002) 551.
[4] U. Ermler, G. Fritzsch, S.K. Buchanan, H. Michel, Structure 2 (1994) 925.
[5] J.P. Allen, G. Feher, T.O. Yeates, H. Komiya, D.C. Rees, Proc. Natl. Acad. Sci. U.S.A. 84 (1987) 5730.
[6] A. Zouni, H.T. Witt, J. Kern, P. Fromme, N. Krauss, W. Saenger, P. Orth, Nature 409 (2001) 739.
[7] N. Kamiya, J.R. Shen, Proc. Natl. Acad. Sci. U.S.A. 100 (2003) 98.
[8] K.N. Ferreira, T.M. Iverson, K. Maghlaoui, J. Barber, S. Iwata, Science 303 (2004) 1831.
[9] N.W. Woodbury, J.P. Allen, in: R.E. Blankenship, M.T. Madigan, C.E. Bauer (Eds.), Anoxygenic Photosynthetic Bacteria, Kluwer Academic Publishers, Dordrecht, 1995, p. 527.
[10] P. Braun, B.M. Greenberg, A. Scherz, Biochemistry 29 (1990) 10376.
[11] V.L. Teten'kin, B.A. Gulyaev, M. Seibert, A.B. Rubin, FEBS Lett. 250 (1989) 459.
[12] P.J.M. van Kan, S.C.M. Otte, F.A.M. Kleinherenbrink, M.C. Nieveen, T.J. Aartsma, H.J. van Gorkom, Biochim. Biophys. Acta 1020 (1990) 146.
[13] B. Löll, J. Kern, W. Saenger, A. Zouni, J. Biesiadka, Nature 438 (2005) 1040.
[14] W. Lubitz, R.A. Isaacson, M.Y. Okamura, E.C. Abresch, M. Plato, G. Feher, Biochim. Biophys. Acta 977 (1989) 227.
[15] P. Moënne-Loccoz, B. Robert, M. Lutz, Biochemistry 28 (1989) 3641.
[16] E. Nabedryk, S. Andrianambinintsova, G. Berger, M. Leonhard, W. Mäntele, J. Breton, Biochim. Biophys. Acta 1016 (1990) 49.
[17] L.B. Giorgi, P.J. Nixon, S.A.P. Merry, D.M. Joseph, J.R. Durrant, J.D. Rivas, J. Barber, G. Porter, D.R. Klug, J. Biol. Chem. 271 (1996) 2093.
[18] S.A.P. Merry, P.J. Nixon, L.M.C. Barter, M.J. Schilstra, G. Porter, J. Barber, J.R. Durrant, D. Klug, Biochemistry 37 (1998) 17439.
[19] K. Cser, I. Vass, Biochim. Biophys. Acta 1767 (2007) 233.
[20] P. Dorlet, L. Xiong, R.T. Sayre, S. Un, J. Biol. Chem. 276 (2001) 22313.
[21] H. Ishikita, J. Biesiadka, B. Loll, W. Saenger, E.W. Knapp, Angew. Chem. Int. Ed. Engl. 45 (2006) 1964.
[22] H. Ishikita, B. Loll, J. Biesiadka, W. Saenger, E.W. Knapp, Biochemistry 44 (2005) 4118.
[23] J. Biesiadka, B. Loll, J. Kern, K.-D. Irrgang, A. Zouni, Phys. Chem. Chem. Phys. 20 (2004) 4733.
[24] S. Lin, A.K.W. Taguchi, N.W. Woodbury, J. Phys. Chem. 100 (1996) 17067.
[25] M.E. van Brederode, R. van Grondelle, FEBS Lett. 455 (1999) 1.
[26] M.H. Vos, J. Breton, J.-L. Martin, J. Phys. Chem. B 101 (1997) 9820.
[27] A.W. Rutherford, in: S.E. Stevens, D.A. Bryant (Eds.), Light Energy Transduction in Photosynthesis: Higher Plant and Bacterial Models, The American Society of Plant Physiologists, Rockville, 1988, p. 163.
[28] A.W. Rutherford, W. Nitschke, in: H. Baltscheffsky (Ed.), Origin and Evolution of Biological Energy Conversion, Wiley-VCH, New York, 1996, p. 143.
[29] J.P. Dekker, R. Van Grondelle, Photosynth. Res. 63 (2000) 195.
[30] V. Prokhorenko, A.R. Holzwarth, J. Phys. Chem. B 104 (2000) 11563.
[31] M. Germano, C.C. Gradinaru, A.Y. Shkuropatov, I.H. van Stokkum, V.A. Shuvalov, J.P. Dekker, R. van Grondelle, H.J. van Gorkom, Biophys. J. 86 (2004) 1664.
[32] B.A. Diner, E. Schlodder, P.J. Nixon, W.J. Coleman, F. Rappaport, J. Lavergne, W.F. Vermaas, D.A. Chisholm, Biochemistry 40 (2001) 9265.
[33] R.N. Frese, M. Germano, F.L. de Weerd, I.H. van Stokkum, A.Y. Shkuropatov, V.A. Shuvalov, H.J. van Gorkom, R. van Grondelle, J.P. Dekker, Biochemistry 42 (2003) 9205.
[34] M.L. Groot, N.P. Pawlowicz, L.J. van Wilderen, J. Breton, I.H. van Stokkum, R. van Grondelle, Proc. Natl. Acad. Sci. U.S.A. 102 (2005) 13087.
[35] A.R. Holzwarth, M.G. Muller, M. Reus, M. Nowaczyk, J. Sander, M. Rögner, Proc. Natl. Acad. Sci. U.S.A. 103 (2006) 6895.

[36] G. Renger, A.R. Holzwarth, in: T.J. Wydrzynski, K. Satoh (Eds.), Photosystem II: The Light-Driven Water: Plastoquinone Oxidoreductase, Springer, Dordrecht, 2005, p. 139.
[37] L.M.C. Barter, D.R. Klug, R. van Grondelle, in: T.J. Wydrzynski, K. Satoh (Eds.), Photosystem II: The Light Driven Water: Plastoquinone Oxidoreductase, Springer, Dordrecht, 2005, p. 491.
[38] A.R. Holzwarth, M.G. Muller, J. Niklas, W. Lubitz, Biophys. J. 90 (2006) 552.
[39] Y. Li, A. van der Est, M.G. Lucas, V.M. Ramesh, F. Gu, A. Petrenko, S. Lin, A.N. Webber, F. Rappaport, K. Redding, Proc. Natl. Acad. Sci. U.S.A. 103 (2006) 2144.
[40] P. Jordan, P. Fromme, H.T. Witt, O. Klukas, W. Saenger, N. Krauss, Nature 411 (2001) 909.
[41] M. Byrdin, P. Jordan, N. Krauss, P. Fromme, D. Stehlik, E. Schlodder, Biophys. J. 83 (2002) 433.
[42] T. Renger, E. Schlodder, in: J.H. Golbeck (Ed.), Photosystem I: the Light-Driven Plastocyan. Ferredoxin Oxidoreductase, vol. 24, Springer, 2006, p. 595.
[43] J.R. Durrant, D.R. Klug, S.L.S. Kwa, R. van Grondelle, G. Porter, J.P. Dekker, Proc. Natl. Acad. Sci. U.S.A. 92 (1995) 4798.
[44] L.M. Barter, J.R. Durrant, D.R. Klug, Proc. Natl. Acad. Sci. U.S.A. 100 (2003) 946.
[45] E. Schlodder, V.V. Shubin, E. El-Mohsnawy, M. Rögner, N.V. Karapetyan, Biochim. Biophys. Acta 1767 (2007) 589.
[46] T. Noguchi, T. Tomo, Y. Inoue, Biochemistry 37 (1998) 13614.
[47] J. Breton, R. Hienerwadel, E. Nabedryk, P. Carmona (Eds.), Spectroscopy of Biological Molecules, Kluwer, Dordrecht, 1997, p. 101.
[48] S.E.J. Rigby, J.H.A. Nugent, P.J. O'Malley, Biochemistry 33 (1994) 10043.
[49] A. Telfer, F. Lendzian, E. Schlodder, J. Barber, W. Lubitz, in: G. Garab (Ed.), Photosynthesis: Mechanism and Effects, vol. 2, Kluwer Academic Publishers, Dordrecht, 1998, p. 1061.
[50] T. Okubo, T. Tomo, M. Sugiura, T. Noguchi, Biochemistry, in press.
[51] G. Raszewski, W. Saenger, T. Renger, Biophys. J. 88 (2005) 986.
[52] V.V. Klimov, S.I. Allakhverdiev, S. Demeter, A.A. Krasnovskii, Dokl. Akad. Nauk SSSR 249 (1979) 227.
[53] A.W. Rutherford, J.E. Mullet, A.R. Crofts, FEBS Lett. 123 (1981) 235.
[54] R.C. Prince, J.S. Leigh, P.L. Dutton, Biochim. Biophys. Acta 440 (1976) 622.
[55] V.A. Shuvalov, I.N. Krakhmaleva, V.V. Klimov, Biochim. Biophys. Acta 449 (1976) 597.
[56] A.W. Rutherford, P. Heathcote, M.C.W. Evans, Biochem. J. 182 (1979) 523.
[57] R.J. Shopes, C.A. Wraight, Biochim. Biophys. Acta 893 (1987) 409.
[58] A. Krieger, A.W. Rutherford, G.N. Johnson, Biochim. Biophys. Acta 1229 (1995) 193.
[59] G.N. Johnson, A.W. Rutherford, A. Krieger, Biochim. Biophys. Acta 1229 (1995) 202.
[60] A. Boussac, A.-L. Etienne, Biochim. Biophys. Acta 766 (1984) 576.
[61] H.J. van Gorkom, Photosynth. Res. 6 (1985) 97.
[62] T.M. Nordlund, W.H. Knox, Biophys. J. 36 (1981) 193.
[63] J.P. Ide, D.R. Klug, W. Kühlbrandt, L.B. Giorgi, G. Porter, Biochim. Biophys. Acta 893 (1987) 349.
[64] B.G. De Grooth, H.J. van Gorkom, Biochim. Biophys. Acta 635 (1981) 445.
[65] F.A. Armstrong, R. Camba, H.A. Heering, J. Hirst, L.J. Jeuken, A.K. Jones, C. Leger, J.P. McEvoy, Faraday Discuss. (2000) 191.
[66] N.W. Woodbury, W.W. Parson, M.R. Gunner, R.C. Prince, P.L. Dutton, Biochim. Biophys. Acta 851 (1986) 6.
[67] P. Sebban, C.A. Wraight, Biochim. Biophys. Acta 974 (1989) 54.
[68] M.R. Gunner, B. Honig, Proc. Natl. Acad. Sci. U.S.A. 88 (1991) 9151.
[69] W. Nitschke, A.W. Rutherford, Biochem. Soc. Trans. 22 (1994) 694.
[70] J. Alric, A. Cuni, H. Maki, K.V. Nagashima, A. Vermeglio, F. Rappaport, J. Biol. Chem. 279 (2004) 47849.
[71] K. Gibasiewicz, A. Dobek, J. Breton, W. Leibl, Biophys. J. 80 (2001) 1617.
[72] W.W. Parson, Z.-T. Chu, A. Warshel, Biochim. Biophys. Acta 1017 (1990) 251.
[73] F. Rappaport, M. Guergova-Kuras, P.J. Nixon, B.A. Diner, J. Lavergne, Biochemistry 41 (2002) 8518.
[74] A. Cuni, L. Xiong, R.T. Sayre, F. Rappaport, J. Lavergne, Phys. Chem. Chem. Phys. 6 (2004) 4825.
[75] D.V. Vavilin, W.F. Vermaas, Biochemistry 39 (2000) 14831.
[76] F. Rappaport, A. Cuni, L. Xiong, R. Sayre, J. Lavergne, Biophys. J. 88 (2005) 1948.
[77] A.M. Nuijs, H.J. van Gorkom, J.J. Plijter, L.N.M. Duysens, Biochim. Biophys. Acta 848 (1986) 167.
[78] G.H. Schatz, H. Brock, A.R. Holzwarth, Biophys. J. 54 (1988) 397.
[79] H.-W. Trissl, W. Leibl, FEBS Lett. 244 (1989) 85.
[80] J. Bernarding, H.-J. Eckert, H.-J. Eichler, A. Napiwotzki, G. Renger, Photochem. Photobiol. 59 (1994) 566.
[81] M. Volk, M. Gilbert, G. Rousseau, M. Richter, A. Ogrodnik, M.E. Michel-Beyerle, FEBS Lett. 336 (1993) 357.
[82] S. Reinman, P. Mathis, Biochim. Biophys. Acta 635 (1981) 249.
[83] B. Hillmann, E. Schlodder, Biochim. Biophys. Acta 1231 (1995) 76.
[84] R. de Wijn, H.J. van Gorkom, Biochim. Biophys. Acta 1553 (2002) 302.
[85] P.J. Booth, B. Crystall, I. Ahmad, J. Barber, G. Porter, D.R. Klug, Biochemistry 30 (1991) 7573.
[86] H. Dau, K. Sauer, Biochim. Biophys. Acta 1273 (1996) 175.
[87] W. Leibl, J. Breton, J. Deprez, H.-W. Trissl, Photosynth. Res. 22 (1989) 257.
[88] M. Grabolle, H. Dau, Biochim. Biophys. Acta 1708 (2005) 209.
[89] D.M. Kramer, C.A. Sacksteder, J.A. Cruz, Photosynth. Res. 60 (1999) 151.
[90] J. Fajer, Photosynth. Res. 80 (2004) 165.
[91] H. Ishikita, W. Saenger, J. Biesiadka, B. Loll, E.W. Knapp, Proc. Natl. Acad. Sci. U.S.A. 103 (2006) 9855.
[92] F. Lendzian, M. Huber, R.A. Isaacson, B. Endeward, M. Plato, B. Bonigk, K. Möbius, W. Lubitz, G. Feher, Biochim. Biophys. Acta 1183 (1993) 139.
[93] A. Ivancich, K. Artz, J.C. Williams, J.P. Allen, T.A. Mattioli, Biochemistry 37 (1998) 11812.
[94] L. Laporte, V. Palaniappan, C. Kirmaier, D.G. Davis, C.C. Schenck, D. Holten, D.F. Bocian, J. Phys. Chem. 100 (1996) 17696.
[95] M. Huber, R.A. Isaacson, E.C. Abresch, D. Gaul, C.C. Schenck, G. Feher, Biochim. Biophys. Acta 1273 (1996) 108.
[96] J.P. Allen, K. Artz, X. Lin, J.C. Williams, A. Ivancich, D. Albouy, T.A. Mattioli, A. Fetsch, M. Kuhn, W. Lubitz, Biochemistry 35 (1996) 6612.
[97] C. Berthomieu, R. Hienerwadel, A. Boussac, J. Breton, B.A. Diner, Biochemistry 37 (1998) 10548.
[98] R. Hienerwadel, A. Boussac, J. Breton, B.A. Diner, C. Berthomieu, Biochemistry 36 (1997) 14712.
[99] M. Sarcina, J. Breton, E. Nabedryk, B.A. Diner, P.J. Nixon, in: G. Garab (Ed.), Photosynthesis: Mechanism and Effects, vol. 2, Kluwer Academic Publishers, Dordrecht, 1998, p. 1053.
[100] A. Camara-Artigas, D. Brune, J.P. Allen, Proc. Natl. Acad. Sci. U.S.A. 99 (2002) 11055.
[101] B.A. Diner, J.A. Bautista, P.J. Nixon, C. Berthomieu, R. Hienerwadel, R.D. Britt, W.F. Vermaas, D.A. Chisholm, Phys. Chem. Chem. Phys. 6 (2004) 4844.
[102] W.F.J. Vermaas, M. Ikeuchi, Y. Inoue, Photosynth. Res. 17 (1988) 97.
[103] K. Brettel, E. Schlodder, H.T. Witt, Biochim. Biophys. Acta 766 (1984) 403.
[104] F. Rappaport, J. Lavergne, Biochim. Biophys. Acta 1503 (2001) 246.
[105] G. Renger, Biochim. Biophys. Acta 1503 (2001) 210.
[106] G. Renger, Biochim. Biophys. Acta 1655 (2004) 195.
[107] F. Rappaport, G. Porter, J. Barber, D. Klug, J. Lavergne, in: P. Mathis (Ed.), Photosynthesis: From Light to Biosphere, Kluwer Academic Publishers, Dordrecht, 1995, p. 345.
[108] M.J. Schilstra, F. Rappaport, J.H.A. Nugent, C.J. Barnett, D.R. Klug, Biochemistry 37 (1998) 3974.
[109] G. Christen, A. Seeliger, G. Renger, Biochemistry 38 (1999) 6082.
[110] G. Christen, G. Renger, Biochemistry 38 (1999) 2068.
[111] R. Ahlbrink, M. Haumann, D. Cherepanov, O. Bögershausen, A. Mulkidjanian, W. Junge, Biochemistry 37 (1998) 1131.
[112] C. Jeans, M.J. Schilstra, D.R. Klug, Biochemistry 41 (2002) 5015.

[113] M.H. Vos, H.J. van Gorkom, P.J. van Leeuwen, Biochim. Biophys. Acta 1056 (1991) 27.
[114] A. Boussac, A.L. Etienne, Biochem. Biophys. Res. Commun. 109 (1982) 1200.
[115] H. Conjeaud, P. Mathis, Biochim. Biophys. Acta 590 (1980) 353.
[116] C.A. Buser, L.K. Thompson, B.A. Diner, G.W. Brudvig, Biochemistry 29 (1990) 8977.
[117] F. Rappaport, J. Lavergne, Biochemistry 36 (1997) 15294.
[118] P. Faller, R.J. Debus, K. Brettel, M. Sugiura, A.W. Rutherford, A. Boussac, Proc. Natl. Acad. Sci. U.S.A. 98 (2001) 14368.
[119] A.W. Rutherford, A. Boussac, P. Faller, Biochim. Biophys. Acta 1655 (2004) 222.
[120] D.A. Campbell, J.M. Peloquin, B.A. Diner, D.A. Chisholm, R.D. Britt, J. Am. Chem. Soc. 119 (1997) 4787.
[121] X.-S. Tang, D.A. Chisholm, G.C. Dismukes, G.W. Brudvig, B.A. Diner, Biochemistry 32 (1993) 13742.
[122] B.A. Diner, R.D. Britt, in: T.J. Wydrzynski, K. Satoh (Eds.), Photosystem II: The light Driven Water: Plastoquinone Oxidoreductase, Springer, Dordrecht, 2005, p. 207.
[123] B.A. Diner, X.-S. Tang, in: P. Mathis (Ed.), Photosynthesis: From Light to Biosphere, Kluwer Academic Publishers, Dordrecht, 1995, p. 229.
[124] G.M. Ananyev, I. Sakiyan, B.A. Diner, G.C. Dismukes, Biochemistry 41 (2002) 974.
[125] C. Jeans, M.J. Schilstra, N. Ray, S. Husain, J. Minagawa, J.H. Nugent, D.R. Klug, Biochemistry 41 (2002) 15754.
[126] M. Sugiura, F. Rappaport, K. Brettel, T. Noguchi, A.W. Rutherford, A. Boussac, Biochemistry 43 (2004) 13549.
[127] I. Vass, S. Styring, Biochemistry 30 (1991) 830.
[128] L.I. Krishtalik, Biochim. Biophys. Acta 849 (1986) 162.
[129] L.I. Krishtalik, Bioelectrochem. Bioenerg. 23 (1990) 249.
[130] J. Lavergne, W. Junge, Photosynth. Res. 38 (1993) 279.
[131] P. Jahns, J. Lavergne, F. Rappaport, W. Junge, Biochim. Biophys. Acta 1057 (1991) 313.
[132] F. Rappaport, J. Lavergne, Biochemistry 30 (1991) 10004.
[133] M. Haumann, W. Junge, Biochemistry 33 (1994) 864.
[134] E. Schlodder, H.T. Witt, J. Biol. Chem. 274 (1999) 30387.
[135] F. Rappaport, M. Blanchard-Desce, J. Lavergne, Biochim. Biophys. Acta 1184 (1994) 178.
[136] M. Haumann, P. Liebisch, C. Muller, M. Barra, M. Grabolle, H. Dau, Science 310 (2005) 1019.
[137] M.R. Razeghifard, R.J. Pace, Biochemistry 38 (1999) 1252.
[138] J. Clausen, W. Junge, Nature 430 (2004) 480.
[139] J. Clausen, W. Junge, H. Dau, M. Haumann, Biochemistry 44 (2005) 12775.
[140] J. Clausen, W. Junge, Photosynth. Res. 84 (2005) 339.
[141] W. Hillier, T. Wydrzynski, Biochemistry 39 (2000) 4399.
[142] T. Wydrzynski, W. Hillier, J. Messinger, Physiol. Plant 96 (1996) 342.
[143] W. Hillier, T. Wydrzynski, Biochim. Biophys. Acta 1503 (2001) 197.
[144] V.P. Shinkarev, C.A. Wraight, Proc. Natl. Acad. Sci. U.S.A. 90 (1993) 1834.
[145] V.P. Shinkarev, Biophys. J. 85 (2003) 435.
[146] B.A. Diner, Biochim. Biophys. Acta 460 (1977) 247.
[147] J. Lavergne, Biochim. Biophys. Acta 682 (1982) 345.
[148] R. de Wijn, H.J. van Gorkom, Photosynth. Res. 72 (2002) 217.
[149] R. de Wijn, T. Schrama, H.J. van Gorkom, Biochemistry 40 (2001) 5821.
[150] J. Lavergne, F. Rappaport, Biochemistry 37 (1998) 7899.
[151] C. Tommos, G.T. Babcock, Biochim. Biophys. Acta 1458 (2000) 199.
[152] J. Barber, G.P. Kraan, Biochim. Biophys. Acta 197 (1970) 49.
[153] C.A. Wraight, A.R. Crofts, Eur. J. Biochem. 19 (1971) 386.
[154] B.A. Diner, P. Joliot, Biochim. Biophys. Acta 423 (1976) 479.
[155] J. Amesz, H.J. van Gorkom, Annu. Rev. Plant Physiol. 29 (1978) 47.
[156] P. Joliot, A. Joliot, Plant Physiol. 65 (1980) 691.